Modelling of Multilayer Perforated Electrodes for Dielectric Elastomer Actuator Applications

by

Seshadri Reddy Nagireddy, Rishabh Bhooshan Mishra, Kumar Sai Charan Karnati, Aftab M Hussain

in

2019 IEEE International Conference on Modeling of Systems Circuits and Devices
(*MOS - AK India 2019*)

IIT Hyderabad, Kandi

Report No: IIIT/TR/2019/-1

Centre for VLSI and Embeded Systems Technology
International Institute of Information Technology
Hyderabad - 500 032, INDIA
February 2019

Modelling of Multilayer Perforated Electrodes for Dielectric Elastomer Actuator Applications

Seshadri Reddy Nagireddy, Rishabh Bhooshan Mishra, Kumar Sai Charan Karnati, Aftab M. Hussain*
Center for VLSI and Embedded System Technologies (CVEST)
International Institute of Information Technology (IIIT) – Hyderabad, Telangana-500032

*Email – aftab.hussain@iiit.ac.in

***Abstract*—A dielectric elastomer actuator (DEA) is a capacitor with an elastomer as dielectric, sandwiched between two complaint electrodes. An electric potential difference applied across the electrodes results in an electric field that creates lateral motion in the device which can be used to perform mechanical work. However, both the dielectric as well as the electrodes needs to be mechanically compliant. In order to achieve high stretchability, carbon nanotube (CNT) based thin films are used as electrodes to maintain conductance even at large mechanical strains. These electrodes are typically fabricated using spray coating or filter transfer method and resemble a perforated electrode under high magnification. Hence, there can be loss of field and stray capacitance when multiple layers of carbon nanotube based electrodes are used. This paper presents theoretical modelling and finite element analysis (FEA) simulations to study the nature of electric field and the effect it has on capacitance of multilayered perforated electrodes for various dimensions and geometric properties of the electrodes. We find that capacitance decreases sharply as the perforation is increased, however, for small uniform perforations (<20%), the decrease in capacitance is found to be negligible (~0.5%). This analysis is important to develop compact models for DEAs for faster simulation of such actuator structures.**

Keywords—Capacitance, perforated electrodes, dielectric elastomer actuator, multilayer DEAs

I. INTRODUCTION

Dielectric elastomer actuators are becoming increasingly relevant in the soft robotics applications [1-4]. These devices rely on electrostatic attraction between oppositely charged complaint electrodes to create mechanical actuation. The compliance of electrodes is necessary for reliable functioning of the actuators because the electrodes need to conduct even when under large mechanical strains. DEAs have been shown to have lateral strains of more than 300% [5], thus the electrodes have to be designed and fabricated such that they maintain their conductance at such a large strain. Further, the electrodes should ideally maintain conductivity after thousands of strain cycles. Several methods of obtaining highly stretchable (or complaint) metal electrodes have been reported in the literature, such as, geometric patterning of electrodes, fabrication of composite electrodes, deposition on compressed thin films and liquid metals [6-11]. However, off these, there are only a few methods that can be used to fabricate the thin-film complaint electrodes usable in a DEA setup. Among them, carbon nanotube based thin films are one of the most used electrode materials for DEA fabrication.

CNTs are one-dimensional, nanoscale (diameter less than 100 nm), cylindrical structures of sp^2 hybridized carbon atoms [12, 13]. They can be thought of as a graphene sheet rolled into a cylindrical shape. Thin films of CNTs consist of a 2D network or a mesh of large amounts of randomly dispersed CNTs. For macroscopic 2D thin films, these networks exhibit conductive behavior similar to a homogenous material. Their conductivity is dependent on the areal density of the CNTs, the dependence being governed by the percolation theory. As such, the conductivity of the thin film increases sharply with the increase in areal density after the areal density exceeds the "percolation limit" for the network [14]. Thereafter, however, the increase in conductivity of the thin film is marginal for a given increase in CNT density. Hence, a minimum areal density of carbon nanotubes is necessary to obtain conduction reliably. On the higher side, the CNT density is constrained by the total stiffness of the thin film. A large stiffness restricts the total displacement obtained from a given DEA structure for a particular applied field. Thus, an optimum CNT density needs to be maintained to obtain highly complaint, low resistance and low stiffness CNT thin films for DEA applications. Fig. 1 shows the motion of a CNT based dielectric elastomer actuator under applied electric field.

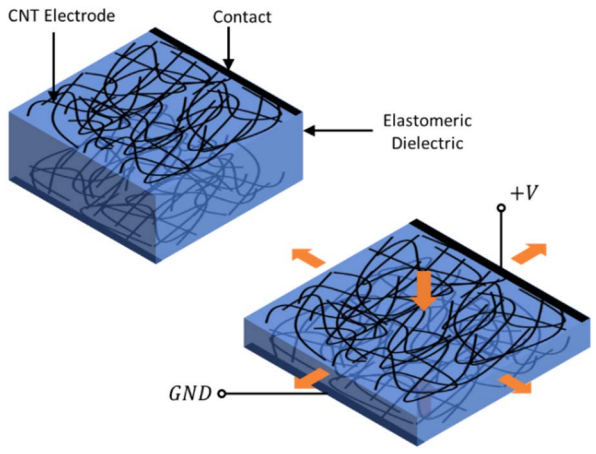

Fig. 1. Schematic illustration of a single layer dielectric elastomer actuator using CNT-based electrodes.

One of the challenges with DEAs is to obtain a large actuating force for a certain applied field. According to DEA theory, the force output depends on the square of the applied voltage, however, voltage cannot be arbitrarily increased

978-1-5386-8007-0/19/$31.00 ©2019 IEEE

because of the breakdown limit of the elastomeric dielectric. Hence, the maximum voltage that can be safely applied to the device is fixed. The force output is thus increased by stacking multiple layers of DEAs on top of each other [15-17]. This increases the output force n times for n layers of stacking. However, this makes the electrostatics of the device more complicated. While macroscopic CNT thin films behave as a homogenous material, at a microscopic level, the film consists of a network of a large number of interwoven CNTs. When a lateral strain is applied, the CNTs merely slide on each other thus increasing the macroscopic dimensions of the network, without losing conductivity, even for large lateral strains. However, this interwoven structure of CNTs does not resemble a continuous thin film but resembles a perforated electrode. This can create complex electric field patterns especially for multilayered DEAs.

In this work, we discuss the nature of the electric fields generated by multilayer perforated electrodes and the corresponding capacitance obtained. In particular, we focus on the screening, or lack of screening, of electric fields created by adjoint capacitors in a multilayer DEA structure, and the effect this has on the observed capacitance of the system. Finally, we show the dependence of the change in capacitance on the dimensions and geometric properties of the electrodes.

II. Compact Modelling of DEAs

DEAs are inherently complaint capacitors. Thus, they can be reasonably represented by a capacitor/resistor model shown in Fig. 2a. The capacitor in the model represents the capacitance of the DEA structure, the series resistor represents the resistance offered by the CNT electrodes and the contact resistance, and the parallel resistor represents the leakage resistance (leakage current) through the dielectric material. However, as discussed in the previous section, the multiple layers of dielectrics and electrodes are fabricated to obtain a larger force output for the same applied electric field. Thus, the model for such multilayer DEAs consist of multiple capacitors connected with a series resistance as shown in Fig. 2b.

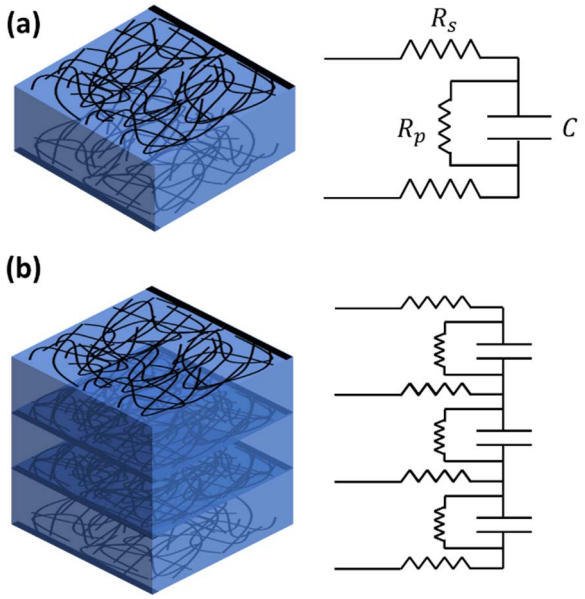

Fig. 2. Capacitor/resistor model for (a) single layer DEA, (b) multilayer DEA.

These capacitors and resistors can be clubbed into single representative capacitor and resistor modeling the complete device behavior. The value of these individual components depends on the fabrication parameters and dimensions. If the metal is assumed to be a continuous thin film, the parallel plate capacitor model can be applied to predict the capacitance of the structure. However, because CNT based electrodes are inherently perforated in nature, the perforations and the resulting distortions in the electric field needs to be taken into account. Thus, it is important to develop models to accurately predict the capacitance exhibited by multilayer DEA structures, particularly while employing perforated electrodes. In the following section, we develop a model to predict the capacitance of a multilayer perforated structure and verify the results using finite element analysis.

III. Modelling Multilayer Capacitor

In general, shielding of electric fields due to the presence of perforated electrodes is a well-known phenomenon. Maxwell introduced some of the trivial cases in his famous Treatise for Electricity and Magnetism [18]. However, detailed calculations of fields can be complicated and require numerical methods to compute.

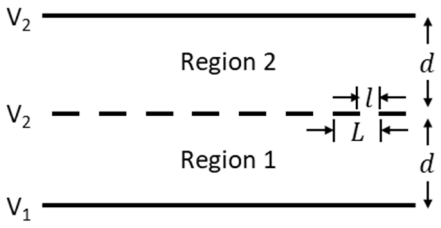

Fig. 3. Schematic illustration of a two-layer capacitance system with perforated central electrode.

Consider the electrode system shown in Fig. 3. The bottom and top electrodes are continuous, while the central electrode is perforated. In the 3D case, the intermediate electrode can be thought of as a collection of parallel stripes of width l and pitch L. A constant voltage V_1 is applied to the bottom electrode, while a constant voltage V_2 is applied to the middle and top electrodes. In case of all solid electrodes, there should be an electric field is Region 1 and no electric field in Region 2. However, in case of a perforated central electrode, Grosser and Schulz have shown that there is an electric field in Region 2 [19], even though the voltages at the central electrode and the top electrode are the same. The fields in both the regions is linearly proportional to the field with all solid electrodes (E_0) and can be mathematically expressed as, $E_1 = (1-\beta)E_0$ and $E_2 = \beta E_0$, where E_1 and E_2 are fields in Region 1 and Region 2 respectively. The constant β depends on the geometry of the perforations of the central electrode and ranges from 0 (in case of no perforations) to 0.5 (in case of no electrode). This relationship is based on the assumption that the electrode perforation dimensions are small compared to the distances and area of the electrodes (thus,$d \gg L$).Further, given this constraint, the electric fields in both the regions will remain almost constant.

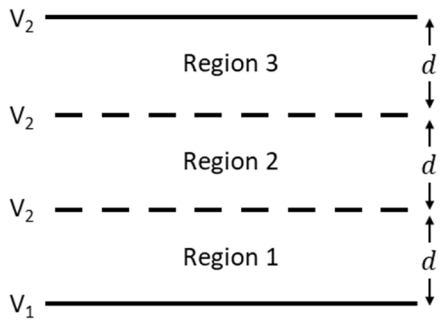

Fig. 4. Schematic illustration fo a three-layer capacitance system with two perforated electrodes.

This result can be extended to the system of four or more electrodes as shown in Fig. 4. Because there exists a constant electric field with in Region 2, according to the previous discussion, it induces a constant electric field in Region 3. Further, because the perforation dimensions are held constant for the intermediate electrodes, the diminishing factor β is also the same for both electrodes. Thus, the resulting field in each case is diminished by a factor of β, thus, $E_1 = (1-\beta)E_0$, $E_2 = (\beta - \beta^2)E_0$, $E_3 = \beta^2 E_0$.

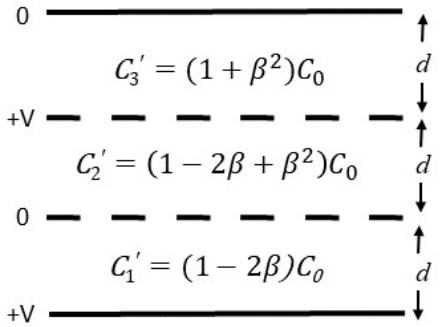

Fig. 5. A three-layer capacitance system with two perforated electrodes with alternate high voltage and ground connections.

In case of multilayer interdigitated capacitors as shown in Fig. 5, the electric fields due to individual structures will superimpose to create the final resultant electric field. Knowing the resultant electric field, and the capacitance of individual structures, the total capacitance can be obtained as the sum of all the capacitors in parallel. Hence, the capacitance for the structure shown in Fig. 5 is given by:

$$C_3 = C_0(3 - 4\beta + 2\beta^2) \tag{1}$$

where, C_0 is the capacitance of a single capacitance with all solid electrodes, and β is the diminishing factor for the electric field because of a perforated electrode. The result can be extended to capacitors of any number of layers. Thus, for an n layer capacitor with uniaxially perforated intermediate electrodes, the resultant capacitance is given by:

$$C_n = C_0[n - 2(n-1)\beta + 2(n-2)\beta^2 - \cdots + 2(-\beta)^{n-1}] \tag{2}$$

Or,

$$C_n = C_0\left(\sum_{i,j=1}^{n}(-\beta)^{|i-j|}\right) \tag{3}$$

where, n is the number of layers in the structure, and C_0 is the capacitance for a single layer capacitor with all solid electrodes.

IV. Simulation Results and Discussion

To verify the analysis, we performed finite element analysis of electric fields using COMSOL Multiphysics. For this analysis we have used Electrostatics Physics Module with stationary study in 2D space domain and obtained capacitance values for various perforation dimensions and layer numbers.

A. Two Dimensional Analysis

The schematic of the capacitor modeled is shown in the Fig. 3, two charged plates are separated by a block of a dielectric. For design of the model, the length of the dielectric was 2000 μm and the thickness was 20 μm. A charged electrode with gaps equally distributed was modeled as a perforated electrode. The electrodes were modelled to be perfectly metallic, while the dielectric block was modelled as a perfect insulator. To simulate the situation in Fig. 3, the top electrode and perforated electrodes were connected to ground, while the bottom electrode was given a voltage 1 V. The electric field distribution obtained is shown in Fig. 6. Ideally, for all solid electrodes, there shouldn't be any electric field in the region between the central and top electrode, however, as shown in Fig. 6, due to perforations of the intermediate electrode, an electric field can be observed. For perforation ratio (l/L) of 0.4, we observed a field leakage of 3%, while for perforation ratio of 0.6, the field leakage is found to be 1%. For perforation ratios greater than 0.6, the field leakage was found to be less than 1%.

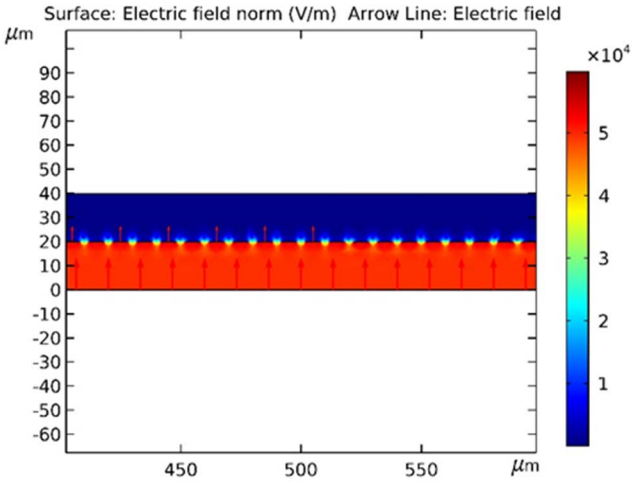

Fig. 6. Finite element analsys (FEA) simulation of a two-layer capacitance system, with bottom electrode at high voltage and top and middle electrode at ground.

In order to proceed with the multilayered analysis, the schematic as shown in Fig. 4 with alternate electrodes at high and ground voltage were modeled. The distance between each electrode was 20 μm and was filled with the dielectric material. Fig. 7 shows electric field of a three-layered capacitance with alternate electrodes at high voltage and ground. The electric field is seen to briefly fringe very close to the perforations. This is expected as there is discontinuity in charge at these points and a high field concentration is expected. At large distances from the perforations, the electric field is seen to be approximately constant as predicted by

Grosser and Schulz. The arrows indicate the alternating direction of the electric field in different regions.

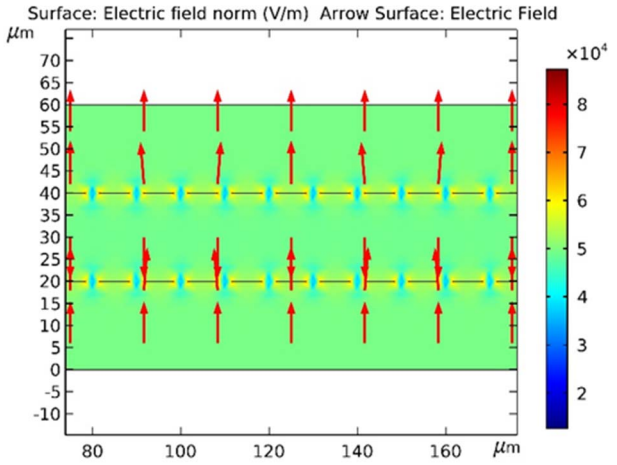

Fig. 7. Finite element analsys (FEA) simulation of a three-layer capacitance system, with alternate electrodes at high voltage and ground.The arrows indicate the direction of the lectric field.

By subsequently adding additional layers to this structure, the structures for higher values of n were obtained. The total capacitance of these multilayered systems was obtained. With the total capacitance for various perforations and layer numbers obtained, we calculated the β for each perforation ratio (l/L). As expected from our analysis, we found that the value of β is independent of the number of layers for a given perforation ratio. Fig. 8 shows the comparison between capacitance obtained from the analytical modelling and that of from simulation, with points representing values calculated using FEA, while the line representing capacitance values calculated using the equations. The values of β were obtained by fitting the curve with the simulated capacitance values. The capacitance values have been normalized to represent the change in capacitance compared with the value of that with all solid electrodes (nC_0). Thus, normalized capacitance (C/nC_0) for all solid electrodes is 1. We observe that for a single layer device, the normalized capacitance is 1 as no perforated electrodes are present. As the number of layers is increased, the normalized capacitance decreases. As expected, the drop in normalized capacitance is more for larger perforation ratios. However, it should be noted that even for a perforation ratio of 0.6, the change in capacitance for seven layers is only 3%.

From Fig. 8 it is evident that for a capacitor with an electrode coverage area of more than 80% (or perforation ratio less than 20%), the normalized capacitance values which are obtained from the FEA analysis are very close to 1.

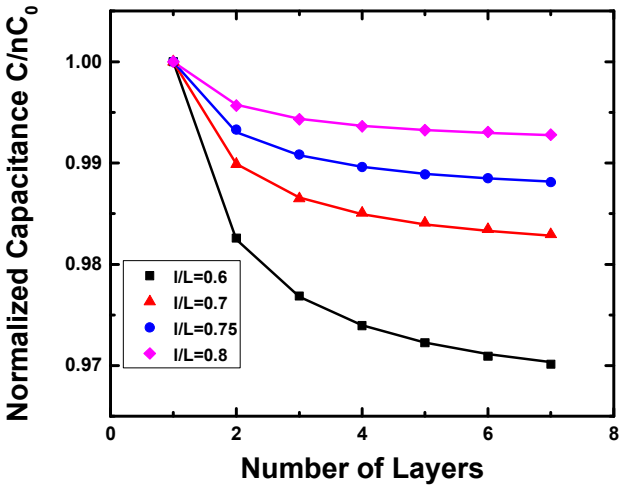

Fig. 8. Normalized capacitance versus number of layers for an interdigitated multilayer capacitance system with perforated intermediate electrodes. The dots represent simulated capacitance values from FEA, while the lines represent capacitance values calculated from theory.

From Fig. 9, for a given layer number, the decline in normalized value of capacitance with perforation ratio is very low. Hence, the areal coverage of CNT electrodes in case of DEAs does not significantly impact the capacitance of the system. For a small value of β, the normalized capacitance can be approximated to the first order as:

$$\frac{C_n}{nC_0} = 1 - 2\beta + \frac{2\beta}{n} \tag{4}$$

As number of layers increases, the normalized capacitance reaches an asymptote at $(1 - 2\beta)$. This result is intuitive, since after a large number of layers, the addition of another layer should not significantly impact the capacitance of layers away from it, thus reducing the effect of number of layers on capacitance of the system. Clearly, as beta goes to zero, i.e., if all the electrodes are completely solid, the normalized capacitance of the system goes to 1.

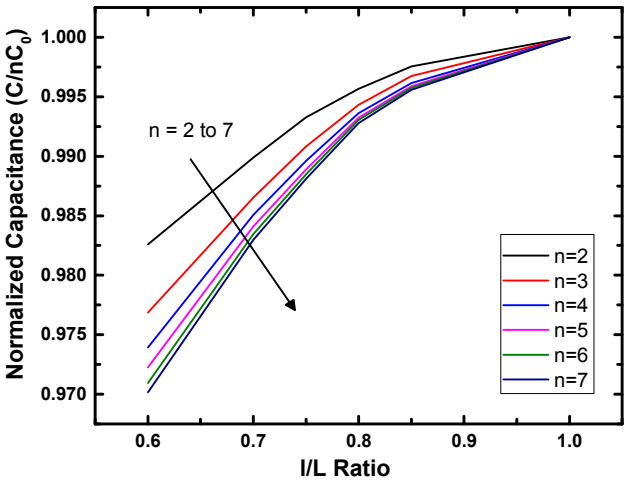

Fig. 9. Variation of normalized capacitance with perforation ratio (l/L) for different number of layers.

V. Conclusion

One of the concerns with using CNTs as electrodes for complaint capacitors, such as DEAs, is the lack of complete areal coverage of the electrode, potentially leading to lower electric fields and lower actuation force. In this work, we have assuaged these concerns by developing an analytical solution for the simple case of lateral perforations with a constant pitch in intermediate electrodes. We present the study of capacitance of multi-layered perforated electrode for DEA applications, using mathematical modelling, and FEA simulation. The study of the multi-layered capacitor includes modelling and simulation of capacitance for various layers and perforation ratios. COMSOL Multiphysics was used to carry out FEA simulations to validate the mathematical modelling of the multi-layered structures. The solution closely matched the theoretical analysis results for normalized capacitance. The analysis and simulations of the capacitor systems suggest that the loss of electric field due to perforations in the electrode system is limited for a reasonable area coverage and can even be neglected for area coverage of more than 80%. The effect of perforated CNT coverage is further diminished with increase in the number of layers.

References

[1] I. A. Anderson, T. A. Gisby, T. G. McKay, B. M. O'Brien, and E. P. Calius, "Multi-functional dielectric elastomer artificial muscles for soft and smart machines," *J. Appl. Phys.*, vol. 112, no. 4, p. 041101, 2012.

[2] S. Shian, K. Bertoldi, and D. R. Clarke, "Dielectric Elastomer Based "Grippers" for Soft Robotics," *Adv. Mater.*, vol. 27, no. 43, pp. 6814-6819, 2015.

[3] H. Zhao, A. M. Hussain, M. Duduta, D. M. Vogt, R. J. Wood, and D. R. Clarke, "Compact Dielectric Elastomer Linear Actuators," *Adv. Functional Mater.*, vol. 28, no. 42, p. 1804328, 2018.

[4] K. Cheng, A. Hussain, and D. Clarke, "Spatially and temporally tunable window devices on flexible substrates," *SPIE Smart Structures and Materials + Nondestructive Evaluation and Health Monitoring*, vol. 10594, p. 8, 2018.

[5] V. Cârlescu, G. Prisăcaru, and D. Olaru, "Electromechanical response of silicone dielectric elastomers," *IOP Conf. Ser.: Mater. Sci. Eng.*, vol. 147, no. 1, p. 012057, 2016.

[6] A. M. Hussain and M. M. Hussain, "CMOS-Technology-Enabled Flexible and Stretchable Electronics for Internet of Everything Applications," *Adv. Mater.*, vol. 28, no. 22, pp. 4219-4249, 2016.

[7] S. Zhu *et al.*, "Ultrastretchable Fibers with Metallic Conductivity Using a Liquid Metal Alloy Core," *Adv. Functional Mater.,* vol. 23, no. 18, pp. 2308-2314, 2013.

[8] A. M. Hussain, F. A. Ghaffar, S. I. Park, J. A. Rogers, A. Shamim, and M. M. Hussain, "Metal/Polymer Based Stretchable Antenna for Constant Frequency Far-Field Communication in Wearable Electronics," *Adv. Functional Mater.,* vol. 25, no. 42, pp. 6565-6575, 2015.

[9] M. D. Dickey, "Stretchable and Soft Electronics using Liquid Metals," *Adv. Mater.*, vol. 29, no. 27, p. 1606425, 2017.

[10] S. Xu *et al.*, "Stretchable batteries with self-similar serpentine interconnects and integrated wireless recharging systems," *Nat. Commun.,* vol. 4, p. 1543, 2013.

[11] A. M. Hussain, E. B. Lizardo, G. A. Torres Sevilla, J. M. Nassar, and M. M. Hussain, "Ultrastretchable and Flexible Copper Interconnect-Based Smart Patch for Adaptive Thermotherapy," *Adv. Healthcare Mater.,* vol. 4, no. 5, pp. 665-673, 2015.

[12] R Saito, G Dresselhaus, MS Dresselhaus, "Raman Spectra of Carbon Nanotubes," in *Physical Properties of Carbon Nanotubes*, World Scientific Publishing, pp. 183-206, 1998.

[13] S. Iijima and T. Ichihashi, "Single-shell carbon nanotubes of 1-nm diameter," *Nature*, vol. 363, p. 603, 1993.

[14] L. Hu, D. S. Hecht, and G. Grüner, "Percolation in Transparent and Conducting Carbon Nanotube Networks," *Nano Lett.*, vol. 4, no. 12, pp. 2513-2517, 2004.

[15] O. A. Araromi, A. T. Conn, C. S. Ling, J. M. Rossiter, R. Vaidyanathan, and S. C. Burgess, "Spray deposited multilayered dielectric elastomer actuators," *Sens. Actuators, A*, vol. 167, no. 2, pp. 459-467, 2011.

[16] A. Punning, S. Akbari, M. Niklaus, and H. Shea, "Multilayer dielectric elastomer actuators with ion implanted electrodes," *SPIE Smart Structures and Materials + Nondestructive Evaluation and Health Monitoring*, vol. 7976, p. 8, 2011.

[17] M. Duduta, R. J. Wood, and D. R. Clarke, "Multilayer Dielectric Elastomers for Fast, Programmable Actuation without Prestretch," *Adv. Mater.*, vol. 28, no. 36, pp. 8058-8063, 2016.

[18] J. C. Maxwell, *A Treatise on Electricity and Magnetism* (no. v. 1). Clarendon Press, 1873.

[19] J. Grosser and H. Schulz, "Electrostatic screening by a plane grid," *J. Phys. D: Appl. Phys.*, vol. 22, no. 6, p. 723, 1989.